

# On the Structural Airworthiness of Fuselages in Presence of Multiple-Site Damage

ICAS-94-8.5.2

Karl-Fredrik Nilsson

The Aeronautical Research Institute of Sweden  
Structures Department

P.O. Box 110 21, S-161 11 Bromma, Sweden

## SUMMARY

A study is made of the effect of small crack damage on the fracture tolerance of an elastic-plastic sheet material to a lead crack. The investigation is motivated by the concern for the influence of multiple-site damage in lap-joints on the tolerance of ageing aircraft fuselages to major cracks. Flat sheet geometries are analysed, unstiffened as well as stiffened ones. Several analysis approaches are explored and assessed, including linear elastic fracture mechanics (LEFM), a modification of LEFM using a damage-reduced fracture toughness, and a modification of the Dugdale model which employs a damage-reduced yield stress of the sheet material. A significant feature of the interaction between a major crack and small crack damage is the fact that the plastic zone of the major crack engulfs several damage sites in geometries typical of most lap-joint designs. The reduction in the average yield-stress in the lap-joint emerges as being the most significant factor in understanding the role of damage, and simple formulas are given which indicate how small crack damage erodes the tolerance of a lead crack.

## NOMENCLATURE

$L$  = tear strap half spacing

$a$  = half length of macro-crack

$w$  = width of tear strap

$h$  = rivet spacing in tear strap

$R$  = Radius of rivet

$a_{MSD}$  = length of micro-cracks

$\sigma$  = applied stress carried by skin

$\sigma_y$  = yield stress of skin

$\sigma_y^{strap}$  = yield stress of strap

$\bar{\sigma}_y$  = averaged yield stress of skin along line of small MSD cracks

$l$  = rivet spacing along lap-joint

$D_{MSD}$  = measure of damage due to MSD-cracks

$K$  = mode I stress intensity factor of major crack in LEFM approach

$K_c$  = mode I toughness of the undamaged skin material

$\delta_i$  = crack tip opening displacement

$\delta_i^c$  = critical value of crack tip opening displacement for crack advance

$s$  = length of plastic zone at major crack tip

## INTRODUCTION

The fuselage of modern aircrafts combine shell skin, stringers, rings and tear straps to provide the pressurized fuselage with a tolerance to major cracks. Traditionally, such design has been based on undamaged lap-joints. The Aloha Airlines accident in 1988 raised the issue to what extent damaged lap-joints in aging aircraft could degrade the tolerance of a fuselage. A particular feature of this damage is the relatively uniform manner in which damage appears at multiple rivet locations, and this form of wide spread fatigue is referred to as *multiple-site damage* (MSD). It is expected by the end of this decade, that 50% of the commercial fleet will exceed their original design life and there is every reason to expect that ageing effects will become an increasing problem. This will most certainly require that future damage tolerance methodologies account for the possibility of MSD. The issue has received considerable attention and overviews of the present state of the art can be found in the proceedings from recent ageing aircraft conferences<sup>1-2)</sup>.

The complexity and the large numbers of parameters render an analysis of the full problem difficult. Simplified models must be relied upon in order to establish an understanding of the dominant effects. One such recent approach considered the interaction between a major crack and small cracks in a flat stiffened sheet by aid of elastic finite element method<sup>3)</sup>. This paper analyses unreinforced and reinforced flat sheets with a major crack and micro-cracks on either side as illustrated in Fig. 1. The residual strength, i.e. the load the structure can sustain, will be assessed using linear fracture mechanics, and more importantly by an approach which accounts for the plastic yielding ahead of the major crack. The fact that plastic effects in the fuselage problem with MSD might be important is obvious when one realizes that the plastic zone length at onset of growth for a typical aircraft sheet material is typically 2 to 4 inches (5-10 cm), depending on the material parameters, whereas the distance between rivets in a lap-joint is typically 1 inch (2.54 cm). The plastic zone of the major crack is therefore sufficiently large to engulf several rivets, and if fatigue damage at the rivets is present, it will

necessarily interact with the plastic zone of the major crack.

The predictions from the linear elastic approach will be contrasted with the predictions from the elasto-plastic model, and the essential role of yielding for the reduction in the residual strength will be demonstrated by examples. A somewhat more detailed discussion on the philosophy and results presented here can be found in <sup>4</sup>.

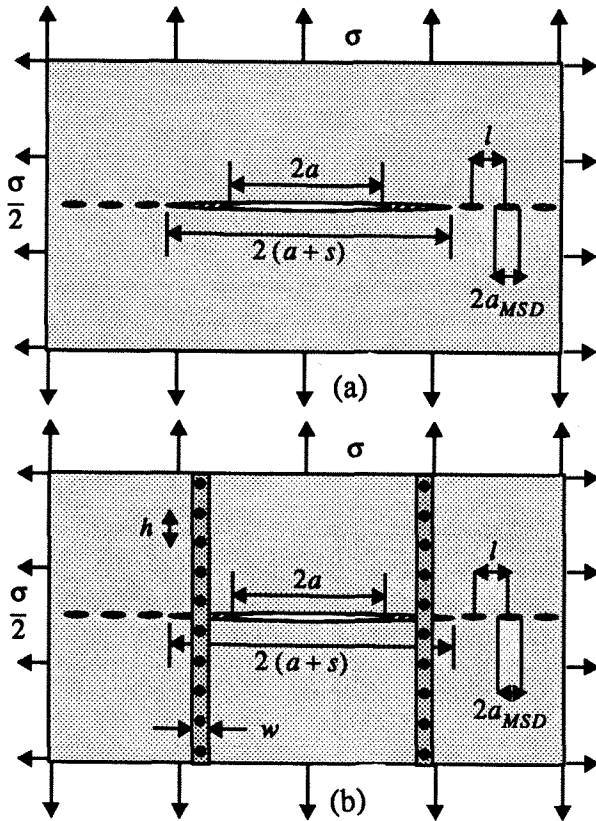


Fig. 1: The Model Problem  
a) Unreinforced sheet with a lead crack and micro-cracks loaded in biaxial tension. b) Reinforced sheet with a lead crack and micro-cracks loaded in biaxial tension.

### PRELIMINARY MODELLING ASPECTS

The sheet material will be modelled as being linearly perfectly plastic with Young's modulus,  $E$ , Poisson's number,  $\nu$ , and with a tensile yield stress,  $\sigma_Y$ . We will in this investigation ignore any crack resistance curve.

### Fracture criteria in the cracked sheet

The linear elastic fracture criterion will assume that the macro-crack can advance when its stress intensity factor,  $K$ , reaches an effective sheet toughness,  $K_c$ . The elastic-plastic criterion for crack advance is based on a critical value of the crack tip opening,  $\delta_i^c$ . It can be shown that for plane stress in the small scale yielding limit, the crack tip opening is uniquely related to the stress intensity factor by  $\delta_i = K^2 / (E\sigma_Y)$ . Thus,  $\delta_i^c$  must be related to  $K_c$  by the same relation, i.e.

$$\delta_i^c = K_c^2 / (E\sigma_Y). \quad (1)$$

The condition  $\delta_i = \delta_i^c$  holds true in both large and small scale yielding, and by virtue of (1) the elastic-plastic approach necessarily reduces to the linear elastic approach in the small scale yielding limit.

### The reduced average tensile yield stress $\bar{\sigma}_Y$ of micro-crack damaged sheet.

Plastic yielding in plane stress may adequately be modelled by a Dugdale zone <sup>5</sup>. It was pointed out above that the plastic zone ahead of a major crack in a typical aluminium sheet material is at least of the order 5-10 cm, engulfing at least 2 to 4 rivets. Any reduction of the ligament area resulting from fatigue cracks at the rivet holes will appear as a corresponding reduction in the plastic limit load capacity of the sheet. In this paper we will imagine that the MSD damage is equivalent to micro-cracks of length  $a_{MSD}$ , and we measure this damage by,  $D_{MSD}$ , defined by

$$D_{MSD} = (l - a_{MSD}) / l. \quad (2)$$

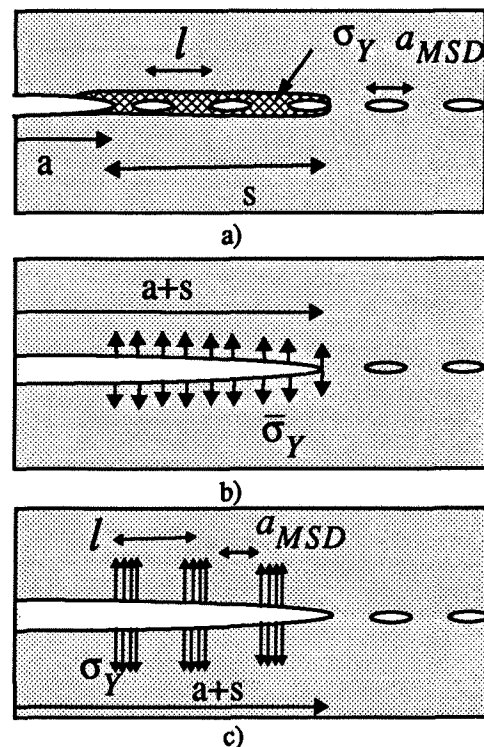


Fig. 2: Weakening of the sheet due to the micro-cracks. a) A schematic illustration of the plastic zone extending from the tip of the major crack in the presence of micro-cracks. b) Weakening as modelled by an average yield stress,  $\bar{\sigma}_Y$ , in the plastic zone  $\bar{\sigma}_Y = \sigma_Y(1 - D_{MSD})$  (Modified Dugdale Model) (c) Ligaments at yield,  $\sigma_Y$ , but crack surfaces traction free in the damage zone ahead of the major crack ("Exact" Dugdale Model).

Fig. 2a illustrates the weakening of the sheet by the micro-crack damage where yielding is localized to a thin strip ahead of the major crack. Fig. 2b and 2c depict two possible ways of modelling this weakening by cohesive zone models.

The "Exact" Dugdale Model represented by Fig. 2c) models the stress distribution exactly for plastic strip ahead of a major crack reaching over traction free micro-cracks, whereas the Modified Dugdale Model smears out the yielding effect by taking an averaged yield stress,  $\bar{\sigma}_Y$ , over the entire plastic strip.

$$\bar{\sigma}_Y = \sigma_Y(1 - D_{MSD}) \quad (3)$$

The Modified Dugdale Model is considerably easier to include in a numerical scheme and it will be shown below that for micro-cracks of equal length, the two models give essentially the same residual strength of the sheet for typical aircraft aluminium sheet materials.

Approximate representation of the micro-cracks outside the plastic zone.

The effect from micro-cracks outside the plastic zone on the lead crack can be accurately modelled by replacing the micro-crack by a dislocation doublet and choosing the amplitude of the doublet's Burgers vector such that the normal stress acting on the doublet centre vanishes<sup>4)</sup>. By this approach the effect from the micro-cracks on the lead crack is determined by simply solving an algebraic linear system of equations.

Representation of tear strap attachment

The rivet forces that transfer forces between the strap and the sheet in Fig. 1b can be computed by assuming displacement compatibility between the strap and the rivet at the attachment points. The concentrated rivet force is applied to the sheet at the centre of the rivet, but the displacement of the sheet in the direction parallel to the strap,  $v$ , is determined as the average displacement in this direction around a circular loop of the rivet radius  $R$  centred at the rivet centre. This is a simpler procedure than employed by for instance Sanders and Bloom<sup>6)</sup>, where the rivets were modelled as "rigid inserts". It can be shown that our approach for representative elastic problems give a difference in the stress intensity factor typically less than 1% compared to the "rigid insert" model.

THE COMPUTATIONAL MODEL

The solution to the model problem can be constructed by the solution to the five sub-problems shown in Fig. 3. The analytical solution to each of the sub-problems can be obtained by using the theory of complex variable methods<sup>7)</sup>. The sub-problem C is not needed for the problem without the tear strap (Fig. 1a) and the sub-problem E is not required in the linear elastic analysis where there is no Dugdale zone, i.e.  $s = 0$ . The plastic zone length  $s$  is

an unknown and is determined from the condition that the normal stress acting across the line just ahead of the plastic zone merges continuously, and falls below,  $\bar{\sigma}_Y$ . This condition is equivalent to a vanishing stress intensity factor at the tip of the extended crack tip.

Due to double symmetry only a quarter needs to be modelled. We describe the computational model for the more complicated elastic-plastic approach of the stiffened sheet.

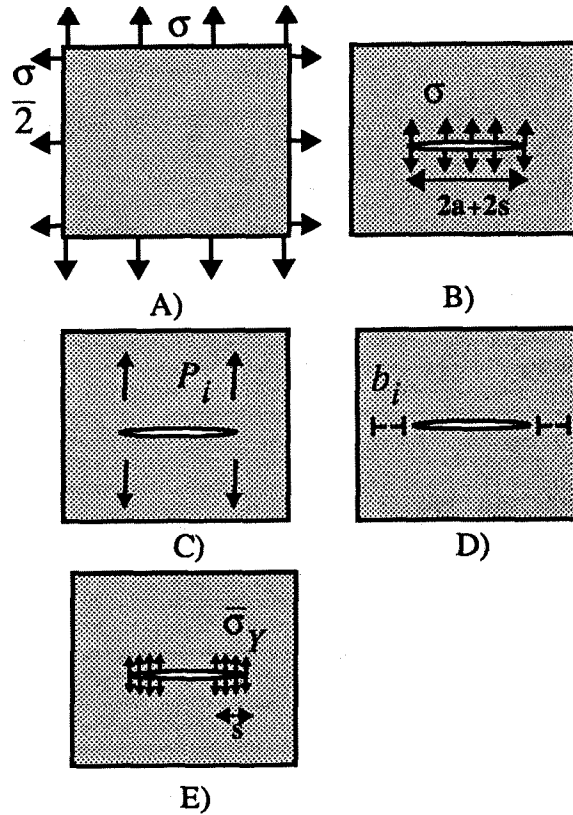


Fig. 3: The five sub-problems required for the Model Problems A) Biaxially loaded sheet B) Cracked sheet loaded with loaded crack surfaces C) Cracked sheet with four symmetry point forces D) Cracked sheet with two symmetric dislocation doublets E) Cracked sheet loads at the end surfaces of the crack.

Assume first that the stress everywhere in the strap is below the yield stress of the strap,  $\sigma_Y^{strap}$ . We also assume that the strap is riveted to the skin. (Bonded tear straps can be accommodated for in an approximate approach by taking sufficiently small distances between rivets.) The unknowns in the problem are the  $N$  amplitudes of the dislocation doublets,  $b_i$ , and the  $M$  point forces,  $P_i$ . Furthermore for a fixed skin stress,  $\sigma$ , the plastic zone length,  $s$ , is also an unknown. There are  $N$  equations corresponding to the requirement that the net normal stress should vanish at the doublet centre. Equilibrium of the tear strap at each of the  $M$  tear strap rivets supply  $M$  equations.

$$(4) \quad \left. \begin{aligned} v_2 - 2v_1 &= -hP_1 / (Ew) \\ v_{i+1} - 2v_i + v_{i-1} &= -hP_i / (Ew) \quad 2 < i < M-1 \\ v_M - v_{M-1} &= -hP_M / (Ew) \end{aligned} \right\}$$

where  $v_i$  is the vertical displacement in the sheet at the  $i$ th tear strap rivet and is expressed in terms of the unknowns. Together these conditions give  $M+N$  linear equations for the doublet strengths and rivet forces.

For an arbitrary value of the plastic zone length,  $s$ , the stresses at the tip of the extended crack ( $x=a+s$ ), will be unbounded and have an inverse square root singularity. The condition that this stress singularity should vanish supplies an equation *linear* in the unknown rivet forces and doublet strengths and the skin stress  $\sigma$ , but *nonlinear* in  $s$ . This suggests that a more effective numerical procedure is to consider the plastic zone length,  $s$ , as known and the skin stress as an unknown. The procedure to find the critical skin stress,  $\sigma_c$ , i.e. the stress at which the crack tip opening displacement reaches its critical value,  $\delta_i = \delta_i^c$ , can be summarized as follows: For a given  $s$  solve the linear system of equation for the  $M+N+1$  unknowns,  $P_i$ ,  $b_i$ , and  $\sigma$ . Compute the associated crack tip opening displacement,  $\delta_i$ , (which depends linearly on the unknowns). Update the plastic zone length and repeat the procedure until the displacement reaches its critical value.

The way to update the plastic zone size is formulated in an iterative procedure, and relatively few iterations are needed to derive  $\sigma_c$ .

The set of equations defined in (4) has to be modified when the strap reaches the yield stress,  $\sigma_Y^{strap}$ . The numerical solution shows that yield is only reached in the segment of the strap bridging the macro-crack, and this particular case is accommodated for by replacing the first equation in (4) with

$$v_2 - v_1 = -hP_1 / (Ew) + h\sigma_Y^{strap} / E \quad (4^*)$$

The strain in the yielded segment is given by  $\epsilon = 2v_1/h$  where  $\epsilon > \sigma_Y^{strap} / E$ . In the case of a broken strap (4\*) is simply replaced by

$$v_2 - v_1 = -hP_1 / (Ew) \quad (4^{**})$$

Otherwise the procedure described above for the elastic strap applies.

#### MATERIAL DATA

The sheet material in the examples below will be assigned material data representative for aluminium 2024-T3 with  $E = 70 \text{ GPa}$ ,  $\nu = 0.33$  and  $\sigma_Y = 345 \text{ MPa}$ . The plane stress fracture toughness,  $K_c$ , has been reported to be  $165 \text{ MPam}^{1/2}$  in some recent tests<sup>8</sup>. This value is somewhat higher than what is usually used. In a

survey by Hoysan and Sinclair<sup>9</sup> values ranging from  $80$  to  $175 \text{ MPam}^{1/2}$  and with a mean value of  $109 \text{ MPam}^{1/2}$  were reported. In this paper we will use  $110$  and  $165 \text{ MPam}^{1/2}$ . The associated crack tip opening displacements are according to (1)

$$\left. \begin{aligned} \delta_i^c &= 1.13 \text{ mm} \quad (K_c = 165 \text{ MPam}^{1/2}) \\ \delta_i^c &= 0.503 \text{ mm} \quad (K_c = 110 \text{ MPam}^{1/2}) \end{aligned} \right\} \quad (5)$$

The small scale yielding estimate of the plastic zone length of the undamaged sheet is

$$\left. \begin{aligned} s &= (\pi/8) (K_c / \sigma_Y)^2 \\ &= 9 \text{ cm} \quad (K_c = 165 \text{ MPam}^{1/2}) \\ &= 4 \text{ cm} \quad (K_c = 110 \text{ MPam}^{1/2}) \end{aligned} \right\} \quad (6)$$

which is larger than the typical rivet spacing ( $2.54 \text{ cm}$ ). The strap material will be assigned material data for the aluminium 7075-T6 reported in<sup>8</sup>,  $\sigma_Y^{strap} = 482 \text{ MPa}$  and with Young's modulus and Poisson's number as given above for 2024-T3.

#### ASSESSMENT OF MODIFIED DUGDALE MODEL

The central idea behind the Modified Dugdale Model shown in Fig. 2b is that the weakening of the sheet material due to micro-cracks can be characterized by the averaged yield stress,  $\bar{\sigma}_Y$ . To assess the accuracy of this model we will compare this model with the "exact" Dugdale model defined in Fig. 2c. In the exact version, zero traction conditions are imposed along the line of small cracks inside the plastic zone and the full yield stress of the sheet material is imposed in between where yielding occurs. Thus, the "exact" Dugdale model treats the micro-cracks as discrete and traction-free entities within the plastic zone. When there is no small crack damage, i.e. when  $D_{MSD} = 0$  is zero, both models reduce to the classical Dugdale model.

Fig. 4a and 4b depict the normalized residual strength for the unstiffened sheets for the damage levels,  $D_{MSD} = 0.1, 0.3, 0.5$  and  $0.75$  with material data as above and using the two alternative models. The distance between the micro-cracks is  $2.54 \text{ cm}$  and this value will be retained in all examples.  $\delta_i^c = 1.13 \text{ mm}$  and  $0.503 \text{ mm}$  in 4a and 4b respectively.

We note that the difference in the result for the two models is small and with the Modified Dugdale Model giving consistently lower residual strength. As expected, the agreement is better for the tougher material for which the plastic zone is larger. From Fig. 4 we conclude that the Modified Dugdale Model seems to be an adequate model for a 2024-T3 aluminium sheet material with a major crack weakened by a large number of identical micro-cracks on each side. The Modified Dugdale will be used in the remainder of this paper.

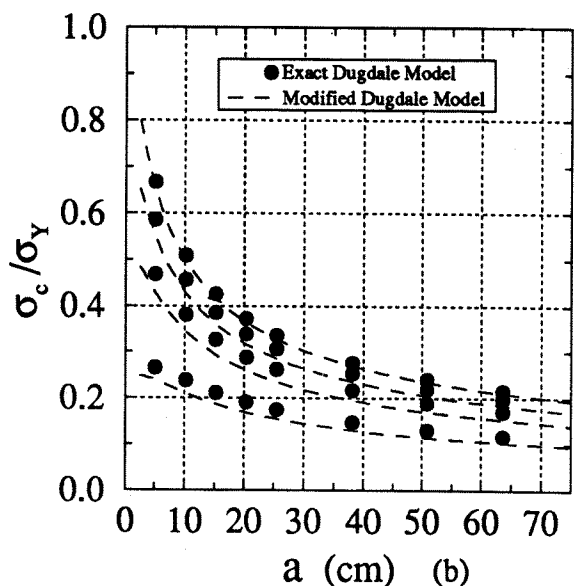
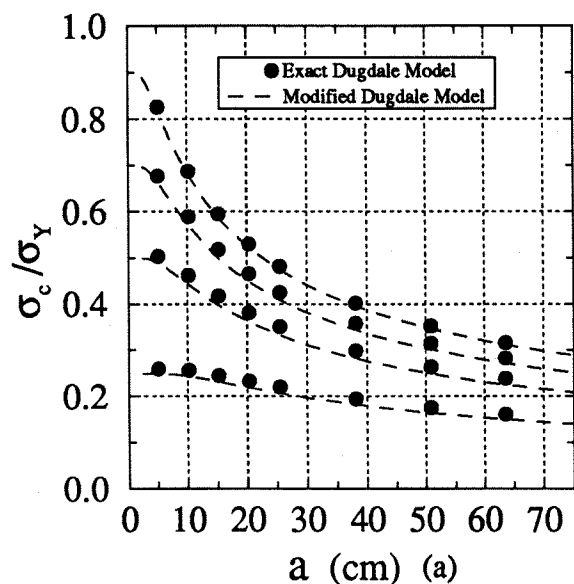


Fig. 4: Residual strength curves for an unstiffened sheet as given by the Modified and "Exact" Dugdale Models respectively for  $D_{MSD} = 0.1, 0.3, 0.5$  and  $0.75$ . a)  $\delta_t^c = 1.13\text{mm}$  b)  $\delta_t^c = 0.503\text{mm}$

#### ELASTIC ANALYSIS VS. THE MODIFIED DUGDALE MODEL FOR THE UNSTIFFENED SHEET

The significance of including the interaction between yielding and the small crack damage is illustrated in Fig. 5 where the residual strength for the unstiffened sheet based on the modified Dugdale is shown together with the linear elastic approach for several damage levels. The linear elastic results are obtained by accounting for the elastic interaction between the major crack and the micro-cracks as discussed earlier with the crack growth criterion  $K = K_c$  imposed to compute  $\sigma_c$ .

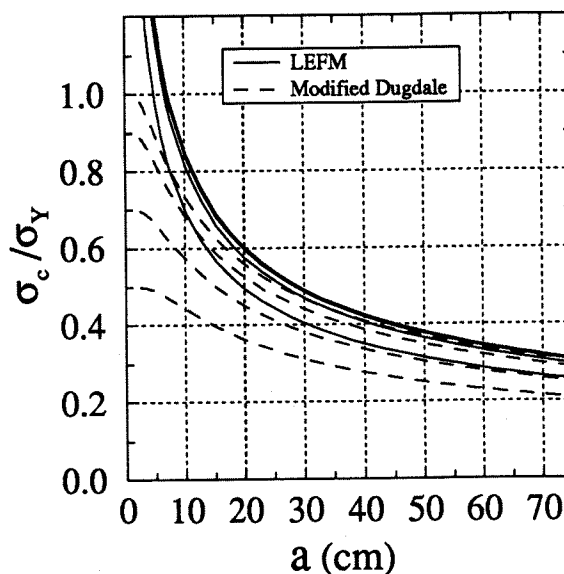


Fig. 5: Residual strength curves for an unstiffened sheet as given by a linear elastic mechanics analysis (LEFM) and the Modified Dugdale Model for  $D_{MSD} = 0, 0.1, 0.3, 0.5$  and  $0.75$ .  $K_c = 165\text{MPa}$   $\delta_t^c = 1.13\text{mm}$

The results are displayed for the higher fracture toughness, i.e.  $\delta_t^c = 1.13\text{mm}$  and  $K_c = 165\text{MPa}$  respectively, but the same pattern is also found for the lower fracture toughness. We note that the difference between the linear elastic and the elasto-plastic approach are small for the undamaged sheet ( $D_{MSD} = 0$ ) except for short cracks where the plastic zone is long compared to the crack length. There is, however, a remarkable difference for the damaged sheet. The linear elastic approach completely fails to capture the significant reduction in the residual strength due to small crack damage. For instance, for the damage level  $D_{MSD} = 0.5$  the elasto-plastic model predicts a reduction in the stress of 35% for long cracks and even more for shorter cracks, whereas the linear elastic approach shows a very small degradation in the residual strength. This simple example epitomizes the fact that micro-crack damage mainly influences the residual strength through plastic interaction.

When the plastic zone size is short compared to the crack length we approach a small scale yielding situation and an equation similar (1) should apply in the limit. This suggests that the micro-crack damage, at least for long cracks, can be modelled in the linear elastic approach by a *damage reduced fracture toughness*. By retaining the condition  $\delta_t = \delta_t^c$  and using (1) it follows that  $\bar{K}_c^2 / (E\bar{\sigma}_Y) = K_c^2 / (E\sigma_Y)$  and from the definition of the damaged reduced yield stress this leads us to a damage reduced critical fracture toughness

$$\bar{K}_c = K_c \sqrt{(1 - D_{MSD})} \quad (7)$$

Thus, by this approach the residual strength is computed from an elastic approach with the elastic crack interaction duly accounted for, but with the fracture criterion  $K = \bar{K}_c$ . Fig. 5 implies that the elastic micro-crack interaction plays a minor role in reduction of the residual strength. This hints to an ever simpler model than (7) to assess the residual strength could be based on the solution for a single major crack in an infinite sheet but adjusted for the reduced fracture toughness,  $\sigma_c = \bar{K}_c / (\sqrt{a\pi})$ . This simple formula together with (7) suggest that the reduction in the critical stress can be assessed by the relationship

$$\sigma_c^{damaged} = \sigma_c^{undamaged} \sqrt{1 - D_{MSD}} \quad (8)$$

where  $\sigma_c^{undamaged}$  is the critical stress for an undamaged sheet based on a linear elastic approach.

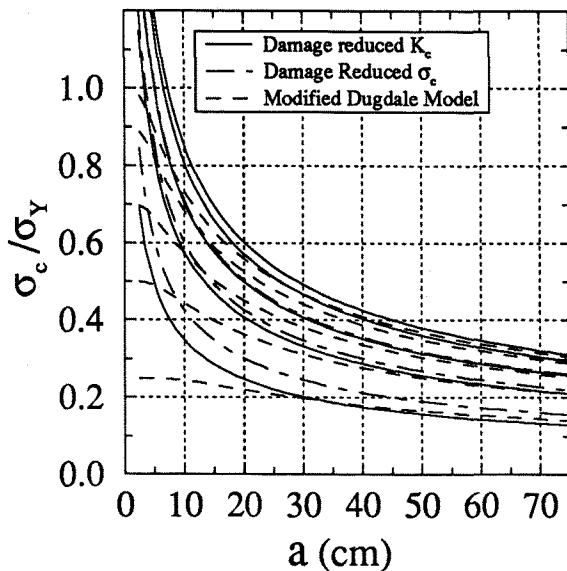


Fig. 6: Residual strength curves for an unstiffened sheet based on (7), (8) and the Modified Dugdale Model respectively for the damage levels,  $D_{MSD} = 0, 0.1, 0.3, 0.5$  and  $0.75$ .

Fig. 6 depicts the residual strength using the approach (7) and (8) respectively together with the modified Dugdale model for the same damage levels as in Fig. 5. The three methods give very similar results for cracks half-lengths exceeding, say, 20 cm. The elastic interaction, which is not included in (8), is only relevant for the highest damage level,  $D_{MSD} = 0.75$ .

#### REINFORCED SHEET CONTAINING A MAJOR CRACK AND SMALL CRACK DAMAGE

An infinite sheet stiffened by two tear straps spaced by a distance 50.8 cm ( $2L$  in Fig 1a) is investigated next. The strap is assumed riveted to the skin with rivet radius,  $R$ , equal to 0.203 cm. The distance,  $h$ , between rivets is

the same as in the lap-joint, i.e. 2.54 cm and the width of the strip,  $w$ , is also 2.54 cm. These values are representative for conventional fuselage designs. As mentioned above, the strap material is taken to be aluminium 7075-T6 with an estimated yield stress,  $\sigma_y^{strap}$ , of 482 MPa. The straps are modelled as elasto-perfectly plastic. The sheet toughness will be  $K_c = 110 \text{ MPa m}^{1/2}$  with the corresponding critical crack tip opening displacement given in (6).

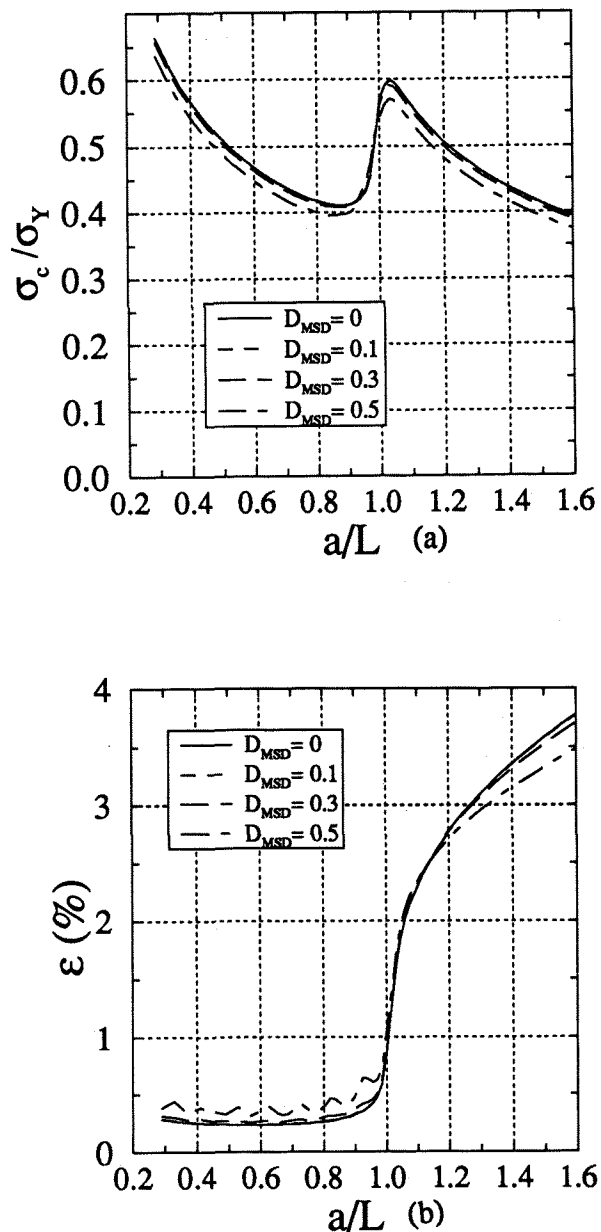


Fig. 7: (a) Residual strength curve for a stiffened sheet as given by a linear elastic fracture model for  $D_{MSD} = 0, 0.1, 0.3$  and  $0.5$  for  $K_c = 110 \text{ MPa m}^{1/2}$  (b) The maximum strain levels in the tear strap associated with the residual strength levels in 7(a).

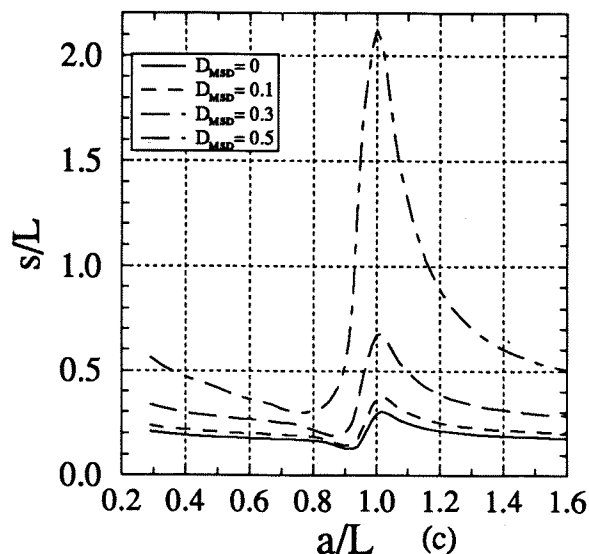
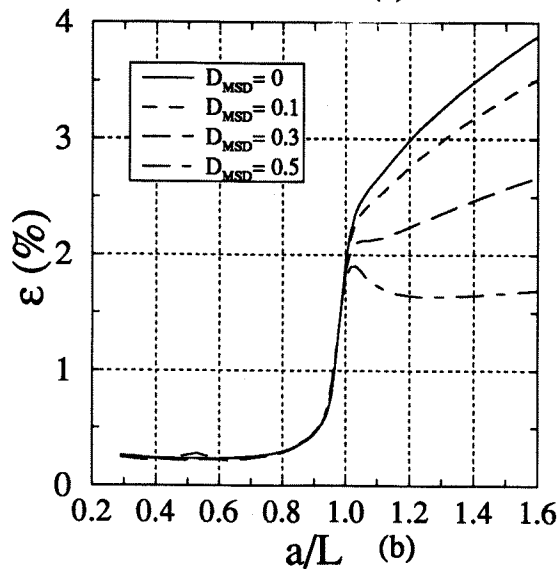
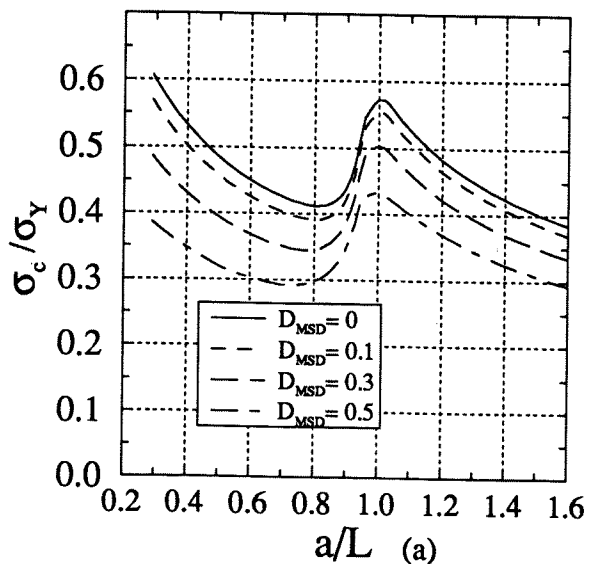


Fig. 8: (a) Residual strength curve for a stiffened sheet as given by a linear elastic fracture model for  $D_{MSD} = 0, 0.1, 0.3$  and  $0.5$  for  $\delta_i^c = 0.503\text{mm}$  (b) The maximum strain levels in the tear strap associated with the residual strength levels in 8(a). (c) Dugdale zone lengths associated with the residual strength levels in 8(a)

The two sets of figures in Fig. 7 display the predicted residual strength and the associated strain level in the segment bridging the crack using the elastic micro-crack interaction. The corresponding predictions based on the Modified Dugdale Model are displayed in Fig. 8 together with the associated plastic zone length. The strap yields when  $\epsilon \geq \sigma_Y^{trap}/E$ , which is  $6.7 \cdot 10^{-3}$  for this particular material, and we note that the strap has yielded before the crack tip has reached the strap. The crack arrest capability is severely over-estimated if yielding of the tear strap is not taken into account

In analogy with the unreinforced sheet, the linear elastic approach predicts only a minor reduction in the residual strength due to micro-crack damage. However, accounting for the micro-crack damage gives a relatively large reduction in the critical stress in the modified Dugdale Model. It is also interesting to note that the residual strength seems to be reduced by approximately the same amount everywhere. Thus, micro-crack damage reduces the overall residual strength, but it does not degrade the crack arrest capability of the straps.

Fig. 9 shows the residual strength for  $D_{MSD} = 0$  and  $0.5$  based on the concept of damage reduced fracture toughness defined by (7) and also the simple formula (8). For reference the modified Dugdale result is also displayed. The reduced fracture toughness concept over-estimates the residual strength considerably when the crack tip reaches the strap (i.e.  $a = L$ ). The simple formula (7) does not account for the plastic interaction from the strap correctly. It is therefore somewhat surprising that the simple formula (7) captures the residual peak stress fairly well.

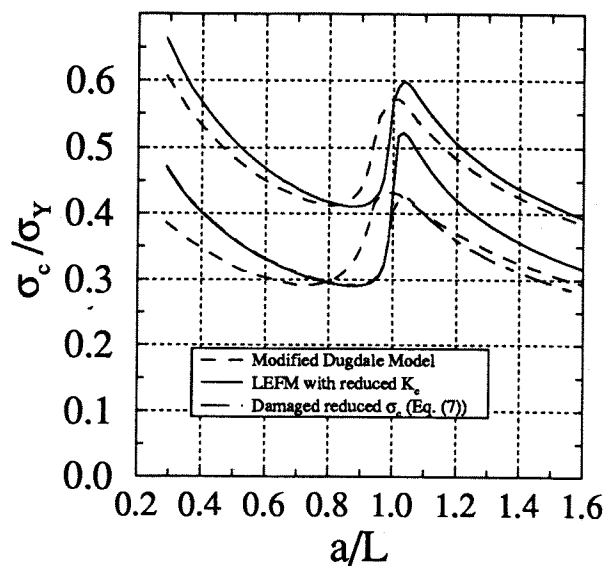


Fig. 9: Residual strength curve as given by the Modified Dugdale Model, LEFM with reduced fracture toughness,  $\bar{K}_c$ , and the damaged reduced critical stress (8) for  $D_{MSD} = 0$  and  $0.5$ .

At high strain levels, the strap will eventually fail and lose most of its crack arrest capability. Fig. 10 shows the residual strength for a broken pair of straps together with the results for an intact strap as in Fig. 8a. At strap failure, the residual strength would drop from the curve represented by the intact strap to the one represented by the broken strap. Given the failure criterion for the strap based on the strap straining, we could predict at which load strap failure occurs. Judging from Fig. 8b the strain level in the strap at the critical stress is not increased by small crack damage and consequently MSD would not precipitate strap failure.

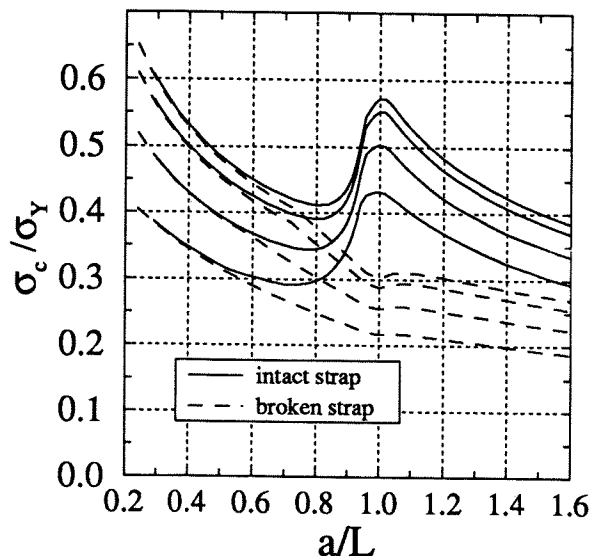


Fig. 10: The residual strength for intact and broken straps of a reinforced sheet using the modified Dugdale Model. The results displayed are for  $D_{MSD}=0, 0.1, 0.3$  and  $0.5$ .

#### CONCLUDING REMARKS

This paper has considered the residual strength of reinforced as well as unreinforced flat sheets with a major crack influenced by small crack damage. The problem has direct bearing on fatigue damaged lap-joints observed in ageing aircrafts where small cracks are distributed along the lap-joint in a relatively uniform manner (MSD). Material data and geometries are chosen in the study to be representative for MSD-damaged fuselages.

A small scale yielding estimate shows that the plastic zone ahead of a major crack at crack advance spans over several damage sites for typical aircraft materials and lap-joint designs. This observation lead us to the conjecture that plastic interaction between the lead crack and the small fatigue cracks plays an important role in how the damage tolerance in such situations is undermined.

The main result of this paper is therefore that the plastic interaction is indeed the single most important factor in understanding how MSD reduces the damage tolerance and it shows up as a reduction in the average yield stress

ahead of the lead crack. By way of examples we show that the failure of the sheet may in these circumstances be successfully analysed by a modification of classical the Dugdale model. Elastic interaction is relatively unimportant and a classical linear elastic fracture mechanics (LEFM) approach will not capture the degradation caused by small crack damage. The concept of LEFM can, however, still be retained to assess residual strength reduction when the lead crack is substantially longer than the plastic zone size by adopting a damage-reduced fracture toughness.

Whether it be for the Modified Dugdale Model or the simpler LEFM-approach with damage-reduced fracture toughness this paper suggests that the predicted damage tolerance reduction is directly related to the damage measured by  $D_{MSD}$ , which directly reflects the fractional reduction in ligament area.

In experiments on curved panels, representative for wide-body fuselages, damage levels ( $D_{MSD}$ ) of order 0.4 reduced the load level by 30% for a major crack. Although the present analysis has dealt with flat panels, it is interesting to note that our predictions are of the same order.

It has been suggested by several authors e.g. <sup>10-11</sup> that a major crack in presence of small crack damage may advance when the first ligament is fully yielded. In my opinion this failure criterion has no rationale in fracture mechanics and it strongly over-estimates the reduction in the residual strength due to small crack damage<sup>11</sup>.

In future work, considerations should be given to strain hardening of the sheet material, and for reliable predictions, crack growth resistance may have to be invoked (R-curve). Such analysis is presently under way<sup>12</sup> in order to analyse flat panels with small crack damage. Secondary bending and effects due to shell curvature, such as bulging are presently considered in work in progress.

#### REFERENCES

- [1] Proceedings from the Int. Workshop on Structural Integrity of Ageing Aeroplanes, Atlanta, 1992, Atlanta Technical Publications. Edited by Atluri, S.N., Sampath, S.G. and Tong, P.
- [2] Proceedings from 5th Int. Conference on Structural Airworthiness of New and Aging Aircraft. 1993, Hamburg. DGLR-Bericht-93-02
- [3] Tong, P. and Greif, R. (1994). Residual strength of aircraft panels with multiple-site damage. *Computational Mechanics*, 13, 285-294.
- [4] Nilsson, K.-F. and Hutchinson, J.W., Interaction between a major crack and small crack damage in aircraft sheet material. Report Mech-215, Harvard University. (1993) (To appear in *Int. Journal of Solids and Structures*)
- [5] Dugdale, D.S., Yielding of Steel Sheets Containing Slits. *J. Mech. Phys. Solids*, 8, 100-104. 1960



- [6] Bloom, J. and Sanders, J.L. (1966), "The effect of a riveted stringer on the stress in a cracked sheet. *J. Appl. Mech.*, 33, 561-570.
- [7] Muskhelishvili, N.I., (1953), *Some basic problems of the mathematical theory of elasticity*. Noordhoff, Holland.
- [8] Samavedam, G. and Hoadley, D., and Thompson, D, (1992) Full scale testing and analysis of curved fuselage panels. Federal Aviation Administration, Department of Transportation, Report DOT-92-01.
- [9] Hoysan, S.F. and Sinclair, G.B. (1993), On the variability of Fracture Toughness. *Int. J. Fracture*, 60, R43-49.
- [10] Swift, T., (1994) Damage Tolerance Capability, *Int. J. Fatigue*, 16, 75-94.
- [11] Broek, D, (1993) The effects of multiple-site damage on the arrest capability of aircraft fuselage structures, *Fracture Research TR 9302*.
- [12] Hutchinson, J.W. and Deng, G. (1994) (private communication)